HHS Public Access

Author manuscript

Eur J Neurosci. Author manuscript; available in PMC 2018 March 01.

Published in final edited form as:

Eur J Neurosci. 2017 March ; 45(5): 733–747. doi:10.1111/ejn.13520.

Disabled-1 dorsal horn spinal cord neurons co-express Lmx1b and function in nociceptive circuits

Griselda M. Yvone, **Hannah H. Zhao-Fleming**, **Joe C. Udeochu**, **Carmine L. Chavez-Martinez**, **Austin Wang**, **Megumi Hirose-Ikeda**, and **Patricia E. Phelps**

Department of Integrative Biology and Physiology, UCLA, Los Angeles, CA 90095

Abstract

The Reelin-signaling pathway is essential for correct neuronal positioning within the central nervous system. Mutant mice with a deletion of Reelin, its lipoprotein receptors, or its intracellular adaptor protein Disabled-1 (Dab1), exhibit nociceptive abnormalities: thermal (heat) hyperalgesia and reduced mechanical sensitivity. To determine dorsal horn alterations associated with these nociceptive abnormalities, we first characterized the correctly positioned Dab1 neurons in wild-type and mispositioned neurons in Reelin-signaling pathway mutant lumbar spinal cord. Using immunofluorescence, we found that 70% of the numerous Dab1 neurons in *Reln*$^{+/+}$ laminae I–II and 67% of those in the lateral reticulated area and lateral spinal nucleus co-express the LIM-homeobox transcription factor 1 beta (Lmx1b), an excitatory glutamatergic neuron marker. Evidence of Dab1- and Dab1-Lmx1b neuronal positioning errors was found within the isolectin B4 terminal region of *Reln*$^{-/-}$ lamina IIinner and in the lateral reticulated area and lateral spinal nucleus, where about 50% of the Dab1-Lmx1b neurons are missing. Importantly, Dab1-Lmx1b neurons in laminae I–II and the lateral reticulated area express Fos after noxious thermal or mechanical stimulation and thus participate in these circuits. In another pain relevant locus – the lateral cervical nucleus, we also found about a 50% loss of Dab1-Lmx1b neurons in *Reln*$^{-/-}$ mice. We suggest that extensively mispositioned Dab1 projection neurons in the lateral reticulated area, lateral spinal nucleus, and lateral cervical nucleus and the more subtle positioning errors of Dab1 interneurons in laminae I–II contribute to the abnormalities in pain responses found in Reelin-signaling pathway mutants.

Graphical abstract

Please address correspondence to: Patricia E. Phelps, Ph.D., Dept. of Integrative Biology and Physiology, UCLA, Terasaki Life Sciences Building, 610 Charles Young Dr. E, Los Angeles, CA 90095-7239, FAX: (310) 206-9184, pphelps@physci.ucla.edu.

Competing interests

The authors declare no competing financial interests.

Author contributions

GMY, HHZF, JCU: designed study, performed experiments, analyzed data, wrote and revised manuscript.
CLCM, AW: analyzed data.
MHI: performed sensory testing.
PEP: designed study, analyzed data, wrote and revised manuscript.

Data Accessibility

We have many large confocal image files that we are willing to share if appropriate.

DR. PATRICIA E PHELPS (Orcid ID : 0000-0003-0735-5341)

Reelin-signaling pathway mutant mice are hypersensitive to thermal and insensitive to mechanical stimulation yet the anatomical abnormalities that cause these alterations are unclear. Here we show that 70% of Disabled-1-expressing dorsal horn neurons in laminae I–II (see image) and lateral lamina V co-express the transcription factor Lmx1b, a marker of glutamatergic neurons. We also found that these Disabled-1-Lmx1b neurons are incorrectly positioned in nociceptive areas of mutant dorsal horns.

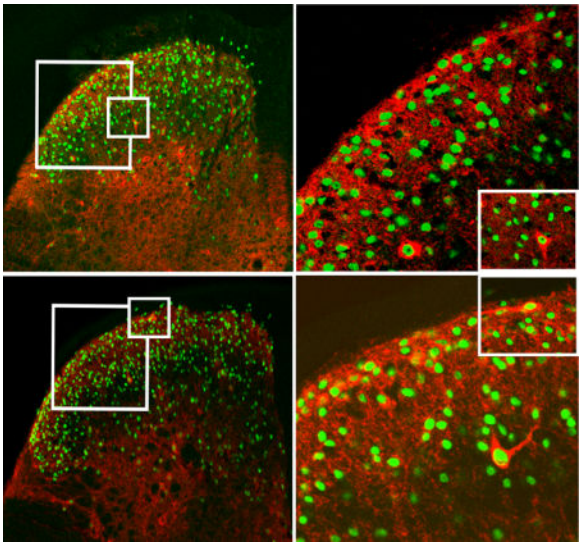

Keywords

Reeler mouse; lateral spinal nucleus; lateral cervical nucleus; pain; neuronal migration disorders

Introduction

During development, the canonical Reelin pathway contributes to the correct positioning of specific neuronal populations, particularly in highly laminated areas including cerebral and cerebellar cortices (Rice *et al.*, 1998; Rice and Curran, 2001; Honda *et al.*, 2011). Reelin is secreted by neurons and binds to two lipoprotein receptors, Apolipoprotein E receptor 2 (Apoer2) and the Very-low-density lipoprotein receptor (Vldlr), which are expressed on nearby neurons. Reelin binding recruits the adaptor protein Dab1 to the intracellular domains of the lipoprotein receptors and stimulates Dab1 phosphorylation by Src-family kinases. This phosphorylation event initiates the downstream signaling necessary for correct neuronal positioning after which migration ceases (Howell *et al.*, 1997; Arnaud *et al.*, 2003; Bock and Herz, 2003). Mice with mutations in various components of the Reelin-signaling pathway produce similar positioning errors in the central nervous system (CNS; Howell *et al.*, 1997; Trommsdorff *et al.*, 1999).

The role of Reelin signaling is extensively studied in higher brain structures, but much less is understood in the spinal cord. Sympathetic and parasympathetic preganglionic neurons in *Reln*$^{-/-}$, *Apoer2*$^{-/-}$/*Vldlr*$^{-/-}$, and *dab1*$^{-/-}$ mice have extensive alterations in their migratory pathways as they fail to stop in their normal lateral locations and instead are found medially

(Yip *et al.*, 2000; Phelps *et al.*, 2002; Yip *et al.*, 2004). In comparison, the somatic motor neurons in *Reln*$^{-/-}$ and *dab1*$^{-/-}$ mice have more subtle positioning errors in the ventral spinal cord (Palmesino *et al.*, 2010; Abadesco *et al.*, 2014).

Previously we reported that *Reln*$^{-/-}$ and *dab1*$^{-/-}$ mice have pronounced dysfunction in pain processing, including increased noxious heat and reduced noxious mechanical sensitivity (Villeda *et al.*, 2006; Akopians *et al.*, 2008; Wang *et al.*, 2012). Despite the extensive functional nociceptive alterations in mutants, the anatomical changes in *Reln*$^{-/-}$ and *dab1*$^{-/-}$ dorsal horns that lead to these abnormalities remain unclear. Information about noxious stimuli is relayed by nociceptors in the dorsal root ganglion to discrete laminae of the superficial dorsal horn (i.e., laminae I–II; Basbaum *et al.*, 2009; Todd, 2010). Some injury messages are transmitted directly via spinal cord projection neurons, whereas most information first engages interneuronal circuits in the dorsal horn; these interneurons, in turn, transmit the information to the projection neurons in the deep dorsal horn and from there to the brainstem and brain (Basbaum *et al.*, 2009; Todd, 2010). Notably, Reelin- and Dab1-expressing neurons are distributed in dorsal horn areas associated with nociception, including the superficial dorsal horn, and two regions containing projection neurons, the lateral reticulated area of lamina V and the LSN (Menétrey *et al.*, 1982; Burstein *et al.*, 1987; Kayalioglu *et al.*, 1999; Kubasak *et al.*, 2004; Villeda *et al.*, 2006; Akopians *et al.*, 2008; Wang *et al.*, 2012). In previous studies, however, we did not identify differences in nociceptor termination patterns in Reelin-signaling pathway mutants (Villeda *et al.*, 2006; Akopians *et al.*, 2008) which suggests that the defects in mutants lie within the dorsal horn circuitry.

To better understand how the disruption of Reelin signaling alters thermal and mechanical nociceptive circuits, we aim to identify the phenotype of Dab1-labeled dorsal horn neurons. Mispositioned Reelin-responsive neurons can be identified in *Reln*$^{-/-}$ by their high levels of Dab1 expression compared to wild-type neurons that continually ubiquitinate and degrade Dab1 (Howell *et al.*, 1997; Rice *et al.*, 1998). Additionally, we will examine a less well-known nociceptive area in cervical levels C1-3, the lateral cervical nucleus (LCN), a region that contains ascending projection neurons involved in thermal and mechanical pain processing (Giesler *et al.*, 1979; Kajander and Giesler, 1987; Burstein *et al.*, 1990). We suspect that the mispositioning of multiple populations of Dab1-positive dorsal horn neurons contributes to the extensive nociceptive abnormalities observed in mutant mice of the Reelin pathway.

Materials and Methods

Animals

***dab1*^{lacZ} mice—**The generation and characterization of *dab1*^{lacZ} mice were described in Pramatarova *et al.* (2008) and Abadesco *et al.* (2014), and mice were obtained from Dr. Brian Howell (SUNY Upstate Medical University, Syracuse, NY). The *dab1*$^{lacZ/+}$ mice have one normal allele that expresses *dab1*, whereas in *dab1*$^{lacZ/lacZ}$ mice, *dab1* expression is eliminated.

***Reln* mice—**We used adult *Reln* mice to investigate Dab1 expression in mutants. The *Reln* (B6C3Fe-ala-*Reln*^{rl}) mice were originally obtained from Jackson Laboratory.

***Reln*$^{rl–Orl}$; *GAD67*^{GFP} mice—**The *Reln*$^{rl–Orl}$ strain was previously described by Takahara *et al.* (1996) and the *GAD67*^{GFP} line was generated by Tamamaki *et al.* (2003). These mice were interbred as described in Abadesco *et al.* (2014) to determine if Dab1 neurons were GABAergic. Genotyping of *dab1*^{lacZ}, *Reln*, and *Reln*$^{rl–Orl}$; *GAD67*^{GFP} mice was adapted from Pramatarova *et al.* (2008), D'Arcangelo *et al.* (1996), and Hammond *et al.* (2006), respectively.

Behavioral tests

All experiments were approved by the Chancellor's Animal Research Committee at UCLA and conducted according to the National Institute of Health guidelines. Earlier studies of *Reln* or *dab1* mice found that their responses did not differ by sex (Villeda *et al.*, 2006; Akopians *et al.*, 2008).

1. Thermal (heat) Hargreaves test—Thermal nociception was examined with the Hargreaves' paw withdrawal test (model 336G stimulator, IITC; Hargreaves *et al.*, 1988). Prior to testing, the optimal intensity of the heat source was determined to be 12% to elicit a 10 sec response from wild-type mice. **Six** males of all three genotypes (*dab1*$^{+/+}$, *dab1*$^{lacZ/+}$, and *dab1*$^{lacZ/lacZ}$) were acclimated in clear plastic tubes for 45 min before the heat source was focused onto the plantar surface of the hind paws for 3 trials each and withdrawal responses were recorded. This model turns off at 20 secs to prevent injury.

2. Thermal (heat) Fos stimulation—Five to seven age-matched sets of female mice, lightly anesthetized with Sodium Pentobarbital (50–60 mg/kg), were used and 15 mins after anesthesia induction, the left hindpaw was dipped into 50°C water for 3 sec/min for 10 min. Due to the inconsistent responses of *dab1*$^{lacZ/+}$ and *dab1*$^{lacZ/lacZ}$ mice to the anesthetic, we set criteria for inclusion into the study. Mice were judged to be over-sedated if they responded to less than 8 of the 10 stimulations or under-sedated if their response to the heat involved exaggerated full body movements. We let such mice recover and re-tested them 1–2 weeks later.

3. Mechanical von Frey test—Five to six male mice **of each genotype** were placed in plastic chambers on an elevated wire mesh for 1 hr before testing with the up-down paradigm of Chaplan (Chaplan *et al.*, 1994). Calibrated von Frey monofilaments (0.008 – 4.0 g) were applied to the center of the plantar surface of the left hindpaw in series, starting with the 0.4 filament. Responses were tabulated and the 50% response for the withdrawal threshold was determined.

4. Mechanical Fos stimulation—Six to seven age-matched male mice from all three genotypes were used and set up as described above for thermal Fos stimulation. The left hindpaw was stimulated with a padded alligator clip for 20 sec every 3 min for a total of 15 min. The same criteria as reported for thermal Fos experiments were used to decide whether to continue with the experiment or re-test later.

Tissue preparation and immunohistochemistry

One hour after noxious stimulation, *dab1*^{lacZ} mice were re-anesthetized (Sodium Pentobarbital, 100 mg/kg) and perfused transcardially with 4% paraformaldehyde, and post-fixed for 1 hour (4°C) in the same fixative. *Reln* and *Reln*$^{rl–Orl}$*;GAD67*^{GFP} mice received the same fixative but with a 1–3 hour post-fix. Following an overnight wash with 0.12M phosphate buffer (PB), spinal cords were dissected and cryoprotected in 30% sucrose/PB for 2–3 days. Upper cervical (C1-3) and lumbar (L4-5) segments were blocked and frozen in Optimum Cutting Temperature (Sakura) and stored at −80°C.

To evaluate Fos expression, we immunostained 5–6 40 μm coronal cryostat sections per mouse lumbar levels 4–5. We used rabbit anti-Fos (1:10,000; Calbiochem, PC38) with 0.1M Tris buffer with 1.4% NaCl and 0.1% bovine serum albumin (TBS). Standard avidin-biotin techniques combined with Nickle-intensified diaminobenzidine were used to visualize Fos expression. Sections were mounted, dried, dehydrated, cleared and coverslipped. Coronal or sagittal sections (25–30 μm) were used for double immunofluorescent experiments.

β-galactosidase histochemistry—Free-floating sections were washed with PB, preincubated for 2–7 h in an X-gal reaction buffer [5 mM $K_3Fe(CN)_6$, 5 mM $K_4Fe(CN)_6$–$3H_2O$, 1 mM $MgCl_2$, 0.01% deoxycholic acid and 0.02% Igepal; Sigma] and reacted in the same buffer plus 1 mg/mL X-gal (Gold Biotechnology) for 1–12 h. After staining, sections were washed with PB and processed for diaminobenzidine immunohistochemistry (Abadesco *et al.*, 2014).

Immunohistochemical procedures—Following β-gal localization, a rabbit antiserum to Dab1 (B3; 1:5,000–1:10,000; generous gift of Dr. Brian Howell; Howell *et al.*, 1997) was used to detect Dab1 protein in free-floating spinal cord sections as in Abadesco *et al.* (2014). Other primary antibodies used include: guinea pig anti-Lmx1b (1:20,000; generous gift of Drs. Müller and Birchmeier; Müller *et al.*, 2002), chick anti-Green Fluorescent Protein (GFP; 1:1,000; Aves Labs, GFP-1020), goat anti-Choline acetyltransferase (ChAT; 1:750; Chemicon, AB144P), mouse anti-Neuronal nuclei (NeuN; 1:900; Millipore, MAB377), and rabbit anti-Neurokinin-1 receptor (NK-1R; 1:8,000; Sigma, S8305). Isolectin B4 (IB4) was visualized using a biotinylated IB4 conjugate (1:200; Vector, B-1205).

Most double or triple-labeling immunofluorescence experiments used the Tyramide Signal Amplification Plus kit (PerkinElmer) as reported (Shields *et al.*, 2010; Abadesco *et al.*, 2014), together with the appropriate biotinylated secondary antibodies. All secondary antibodies were purchased from Jackson Immunoresearch. Those used at a 1:500 dilution were donkey anti-chick Alexa Fluor 488, and biotinylated donkey anti-mouse or rabbit for diaminobenzidine reactions. Streptavidin Alexa Fluor 488 (1:1,000) was used for the IB4 conjugate. For Dab1-Fos-Lmx1b triple labeling, citric acid treatment was performed as described in Abadesco *et al.* (2014) to co-localize two rabbit antisera, i.e. Dab1 and Fos.

A Zeiss Laser Scanning Microscope (LSM510) was used to obtain thin confocal images of the immunofluorescent co-localization as stated in the figure legends. Low magnification confocal images were obtained with 10×, and high magnification images, with a 40× objective. Each confocal image represents a 3 μm thick slice except for those of the lateral

reticulated area and LSN. Due to the small number of neurons present in these two areas, their 3 μm slices were collapsed into a single image. Fluorescent and brightfield images were collected with a Zeiss AxioCam HRc camera on an Olympus AX70 microscope. Images were analyzed with LSM Image browser, and then transferred to Photoshop for assembly, cropping, and adjustment of brightness and contrast.

Statistical Analyses

Fos stimulation and behavioral studies—Five to six hemisections per mouse with the highest number of Fos-localized cells were photographed and analyzed. Laminae I–II, III–IV, V–VI, and the LSN were delineated and Fos-positive cells/area counted as in Wang *et al.* (2012). The means of Fos-positive cells were compared by genotype and spinal area using a 3 × 4 repeated measures two-way analysis of variance (ANOVA) model where the spinal area is the repeated within-group factor and genotype is the between-group factor. Under this ANOVA model, *post hoc* mean comparisons were judged significant using the Fisher least significant difference criterion unless specified. For the Hargreaves test, mean values were evaluated with ANOVA. For the von Frey test, significance of the mean threshold values was evaluated with the Kruskal-Wallis test. Calculations were carried out with JMP 10 (SAS Inc.) or Sigma Plot 12.0 (Systat Software Inc.), respectively.

Mispositioning and Dab1-Lmx1b co-localization analyses—Coronal sections at lumbar 4–5 levels were imaged with confocal microscopy. Between 5–7 hemisections per mouse from 4–5 *Reln* pairs were analyzed. Cell counting in the superficial dorsal horn was carried out in a single 3 μm confocal slice. The superficial dorsal horn and LSN were determined as in Wang *et al.* (2012). The delineation of the LCN/LSN in cervical levels C1-3 is shown in the LCN figure. Cells in the lateral reticulated area of lamina V were counted in a box (17000 μm × 17000 μm) drawn on the 40× confocal image with the LSN as the lateral border. The means of Dab1- and Dab1-Lmx1b-labeled cells were compared by genotype and/or area for each cell type with a 1 × 2 or 2 × 2 repeated measures two-way ANOVA and *post-hoc* t-tests. Significance of other analyses including IB4 area measurements, NeuN and NK-1R width for the LCN/LSN were determined using ANOVA and *post-hoc* t-tests. Calculations were done using Microsoft Excel or with JMP 10 (SAS Inc.).

Results

The *dab1*$^{lacZ/lacZ}$ mice have increased thermal sensitivity and enhanced Fos expression

Before characterizing the dorsal horn in *dab1*^{lacZ} mice, we asked if the nociceptive behavior of *dab1*$^{lacZ/+}$ mice was comparable to *dab1*$^{+/+}$ and if *dab1*$^{lacZ/lacZ}$ mice displayed nociceptive abnormalities typical of other Reelin-signaling pathway mutants. Results from the Hargreaves test of thermal sensitivity found no differences in the withdrawal latencies between *dab1*$^{+/+}$ and *dab1*$^{lacZ/+}$ mice, whereas *dab1*$^{lacZ/lacZ}$ mice had a significantly shorter latency (Fig. 1A).

We used Fos expression following noxious heat stimulation as a marker of neuronal activity and found no differences between the number of Fos-labeled cells in the *dab1*$^{+/+}$ and

dab1$^{lacZ/+}$ dorsal horns (Fig. 1B). The *dab1*$^{+/+}$ and *dab1*$^{lacZ/+}$ laminae I–II had fewer Fos-labeled cells than in *dab1*$^{lacZ/lacZ}$ mice (Fig. 1B–E). However, in the *dab1*$^{+/+}$ and *dab1*$^{lacZ/+}$ LSN (Fig. 1C–E, short arrows), there were more Fos-labeled nuclei than in *dab1*$^{lacZ/lacZ}$ mice (Fig. 1B–E). These somewhat contradictory findings can be explained by the 50% reduction in the number of neurons in the LSN of Reelin-signaling pathway mutants (Villeda *et al.*, 2006; Akopians *et al.*, 2008). Individual observations of the *dab1*$^{+/+}$ and *dab1*$^{lacZ/+}$ lateral reticulated area (Fig. 1C–E, long arrows) frequently had more Fos-expressing cells than those of *dab1*$^{lacZ/lacZ}$ mice, but the total cell numbers did not differ when evaluated in combination with laminae V-VI (Fig. 1B–E). Overall, our results confirm that *dab1*$^{lacZ/lacZ}$ mice display thermal hyperalgesia, as found in other Reelin-signaling pathway mutants (Villeda *et al.*, 2006; Akopians *et al.*, 2008).

Reduced mechanical sensitivity and Fos expression characterize *dab1*$^{lacZ/lacZ}$ mice

Results from the Chaplan up-down test of mechanical sensitivity found no differences in the 50% withdrawal latencies between *dab1*$^{+/+}$ and *dab1*$^{lacZ/+}$ mice (Fig. 1F). The *dab1*$^{lacZ/lacZ}$ mice, however, had much higher mechanical thresholds (Fig. 1F). After noxious mechanical stimulation the number of Fos-labeled cells did not differ between the *dab1*$^{+/+}$ and *dab1*$^{lacZ/+}$ dorsal horns (Fig. 1G), whereas the *dab1*$^{lacZ/lacZ}$ mice had fewer Fos-expressing cells in laminae I–II and LSN (Fig. 1G–J, short arrows). Again, Fos-labeled neurons in *dab1*$^{+/+}$ and *dab1*$^{lacZ/+}$ lateral reticulated area were greatly reduced in *dab1*$^{lacZ/lacZ}$ mice (Fig. 1H–J, long arrows). These results support our previous findings on reduced mechanical pain sensitivity in *Reln* and *dab1* mutants (Villeda *et al.*, 2006; Akopians *et al.*, 2008; Wang *et al.*, 2012).

Dab1 expression in the adult dorsal horn

As mutations in the Reelin pathway cause abnormalities in neuronal positioning, we then characterized Dab1 expression in adult dorsal horn using a combination of β-gal histochemistry and Dab1 immunohistochemistry. In the superficial dorsal horn, it is difficult to distinguish Dab1-expressing neurons due to extensive terminal staining. Dab1 expression in *dab1*$^{+/+}$ appeared as diffuse reaction product and a few discernible neurons (small arrowheads in Fig. 2A). Several Dab1 cells are detected in laminae III–IV, while the lateral reticulated area of lamina V has a number of medium and a few large Dab1-labeled neurons (large arrowheads in Fig. 2A). The LSN contained strong Dab1 reaction product and a few labeled cells.

In the *dab1*$^{lacZ/+}$ dorsal horn, the β-gal reaction product and Dab1 immunoreactivity are found within the same areas and co-localize within cells of the lateral reticulated area (Fig. 2B and inset), confirming that both methods identify the same neurons. As expected, the *dab1*$^{lacZ/lacZ}$ dorsal horn contained only β-gal deposits which were concentrated in laminae I–II and the lateral reticulated area (Fig. 2C), similar to the protein expression pattern in *dab1*$^{+/+}$ dorsal horn (Fig. 2A). Because β-gal deposits are not found in axons of Dab1 neurons (Abadesco *et al.*, 2014), the heavy β-gal product in the superficial dorsal horn suggests that there are many more Dab1-labeled neurons than we previously reported (Villeda *et al.*, 2006; Akopians *et al.*, 2008). The heterogeneity in size and regional

distribution suggests that Dab1 is widely expressed in several distinct dorsal horn populations.

Superficial dorsal horn: most Dab1 cells co-express the transcription factor *Lmx1b*

Next we sought to identify the phenotype of the **small** Dab1 neurons in laminae I–II **that resemble the classically defined nociceptive-specific dorsal horn neurons.** Because the majority of interneurons in this area are excitatory (Todd, 2010), we asked whether they were glutamatergic neurons. There are two homeobox proteins, Lmx1b and Tlx3 (T-Cell Leukemia Homeobox 3), that mark a late-generated dorsal neuron population (dIL^{B}) that migrates to the superficial laminae of the dorsal horn and differentiates into an excitatory glutamatergic phenotype (Gross *et al.*, 2002; Müller *et al.*, 2002; Cheng *et al.*, 2004; Cheng *et al.*, 2005; Dai *et al.*, 2008; Rebelo *et al.*, 2010). Because Lmx1b expression is maintained in adults (Dunston *et al.*, 2005; Dai *et al.*, 2008), we asked if Dab1 dorsal horn neurons express Lmx1b. The β-gal product was detected in the same $dab1^{lacZ/+}$ and $dab1^{lacZ/lacZ}$ dorsal horn areas as Lmx1b (data not shown). To better identify the Dab1-expressing neurons, we conducted double immunofluorescence experiments, confocal imaging and extensive analyses on $Reln^{+/+}$ and $Reln^{-/-}$ dorsal horns and confirmed Dab1 and Lmx1b co-localization (Fig. 3A–F). Analyses of 3 μm confocal images revealed that 70% of the small to medium Dab1-expressing superficial dorsal horn neurons co-express Lmx1b (yellow arrowheads in Fig. 3B, B1-2, E, E1-2; $Reln^{+/+}$ 71±2%; $Reln^{-/-}$ 70±2%). Compared to $Reln^{+/+}$, there are a few medium and large-sized Dab1-Lmx1b neurons in $Reln^{-/-}$ laminae I–II (Fig. 3F; compare Fig. 3A to D and Fig. 3G to H) and dorsal funiculus (**data not shown**). Based on previous studies (Cheng *et al.*, 2004; Cheng *et al.*, 2005; Dai *et al.*, 2008), the Dab1-Lmx1b neurons are likely to be glutamatergic.

We also tested other common markers of excitatory superficial dorsal horn neurons (Antal *et al.*, 1991; Todd, 2010; Gutierrez-Mecinas *et al.*, 2016). Although many Protein Kinase C gamma (PKCγ)-positive interneurons express Lmx1b, none of the Dab1-labeled neurons co-expressed PKCγ (data not shown). The Dab1 neurons also did not express Calretinin, but a few Dab1-Lmx1b neurons did contain Calbindin and Somatostatin (data not shown). Additionally, our previous studies showed that a few Dab1 dorsal horn neurons expressed the Neurokinin-1 receptor that binds substance P and were mispositioned in Reelin-signaling pathway mutant dorsal horns (Villeda *et al.*, 2006; Akopians *et al.*, 2008). We conclude that most of the Dab1 neurons in the superficial dorsal horn are excitatory glutamatergic neurons.

Superficial dorsal horn: Dab1-Lmx1b-expressing neurons are mispositioned in *Reln*$^{-/-}$ mice

As mispositioned neurons in $Reln^{-/-}$ mice express high levels of Dab1, we compared the distribution of Dab1 and Dab1-Lmx1b neurons in $Reln^{+/+}$ and $Reln^{-/-}$ superficial dorsal horn. Initial analyses divided laminae I–II into equal-sized bins in both the mediolateral and dorsoventral divisions, but the number of Dab1 neurons per bin did not differ between genotypes.

Because the superficial dorsal horn lamination pattern is precisely defined by primary afferent terminations, we next focused our analysis on lamina IIinner, which is marked by

isolectin B4 (IB4) and receives nonpeptidergic nociceptive afferents (Basbaum *et al.*, 2009; Todd, 2010). Although the area identified by IB4-positive afferents did not vary by genotype, we found fewer Dab1-only (*Reln*$^{+/+}$ 4±0.4; *Reln*$^{-/-}$ 8±1; p=0.002, Fig. 3I) and Dab1-Lmx1b neurons (*Reln*$^{+/+}$ 13±2; *Reln*$^{-/-}$ 18±2; p=0.043, Fig. 3I) in the *Reln*$^{+/+}$ than *Reln*$^{-/-}$ IB4 region. Additionally, the IB4 band in *Reln*$^{-/-}$ lamina IIinner appeared shifted dorsally and perhaps laterally (Fig. 3G–H). Consistent with the more dorsal location of IB4-positive terminals, the area of laminae I–II outer was larger in *Reln*$^{+/+}$ than in *Reln*$^{-/-}$ mice (*Reln*$^{+/+}$ 17,444± 1,357 μm^2; *Reln*$^{-/-}$ 11,264± 978 μm^2; p=0.002, Fig. 3G–H). Despite the reduced area in *Reln*$^{-/-}$ laminae I–II outer, the number of Dab1 cells in this area did not vary by genotype (Fig. 3I). To verify that the Dab1 cells did not die selectively in *Reln*$^{-/-}$, we compared total Dab1 neurons per 3 μm hemisections of *Reln*$^{+/+}$ (65±14 neurons) and *Reln*$^{-/-}$ (77±11 neurons) mice and found no significant difference (p=0.15). Thus the Dab1- and Dab1-Lmx1b-labeled **laminae I–II** neurons, and the IB4-positive terminals **all** appear to be mispositioned in *Reln*$^{-/-}$ superficial dorsal horn.

Superficial dorsal horn: several Dab1 neurons are GABAergic

After finding that 70% of the Dab1 superficial dorsal horn neurons are excitatory, we asked if the other Dab1 neurons in laminae I–II might be inhibitory and express glutamic acid decarboxylase (GAD67). To best answer this question, we used *Reln*$^{rl-Orl}$ mice interbred with a well-characterized *GAD67*^{GFP} line that expresses GFP under the GAD67 promoter (Tamamaki *et al.*, 2003; Abadesco *et al.*, 2014). The majority of GAD67^{GFP}-labeled neurons did not co-localize with Dab1 in *Reln*$^{rl-Orl/+}$ or *Reln*$^{rl/Orl/rl-Orl}$ superficial dorsal horn (Fig. 4A–D). A few double-labeled neurons were present, however, in laminae I–II (yellow arrowheads in Fig. 4B, B1-2, D, D1-2). We also observed Dab1 and Dab1-GAD67^{GFP} neurons in the white matter dorsal to lamina I in *Reln-Orl*$^{+/+}$ (Fig. 4E1-3) and *Reln*$^{rl/Orl/rl-Orl}$ (Fig. 4F1-3) sagittal sections. More large Dab1-immunoreactive neurons appeared to be located in *Reln*$^{rl/Orl/rl-Orl}$ than in *Reln-Orl*$^{+/+}$ superficial dorsal horn (Fig. 4F1, 3 vs 4E1, 3). Markers of subsets of GABAergic dorsal horn interneurons, such as those that express neuronal nitric acid synthase, Parvalbumin, and ChAT also were tested and did not co-localize with Dab1 cells (Fig. 4G–H; data not shown; Laing *et al.*, 1994). We conclude that relatively few Dab1 neurons are inhibitory.

Lateral reticulated area and LSN: Dab1-Lmx1b neurons are mispositioned in *Reln*$^{-/-}$ mice

Previously we found Dab1 neurons in the lateral reticulated area of lamina V, an important nociceptive area containing projection neurons for which few markers have been identified. Here we asked if the Dab1 neurons in the lateral reticulated area also express Lmx1b and found that 67% of Dab1 neurons co-express Lmx1b in both genotypes (Fig. 5A, yellow arrowheads in Fig. 5C, C1-2, E, E1-2). We then analyzed both Dab1- and Dab1-Lmx1b-labeled neurons to look for evidence of neuronal positioning errors in *Reln*$^{-/-}$ mice. Greater numbers of Dab1-Lmx1b neurons are found in the *Reln*$^{+/+}$ (4±0.4) than in *Reln*$^{-/-}$ lateral reticulated area (2±0.3; p=0.0004, Fig. 5G), whereas fewer single-labeled Dab1 neurons are present in *Reln*$^{+/+}$ (2±0.3) than *Reln*$^{-/-}$ mice (4±0.6; p=0.002, Fig. 5G). Several cholinergic neurons in the lateral reticulated area (Phelps *et al.*, 1984) also expressed Dab1 in *Reln*$^{+/+}$ and *Reln*$^{-/-}$ mice (yellow arrowheads in Fig. 4G1-3 and 4H1-3), but due to the small number of double-labeled cells, positioning errors were not evaluated.

As with other Reelin pathway mutants, we recorded about 50% more NeuN-labeled neurons in the LSN of *dab1*$^{+/+}$ and *dab1*$^{lacZ/+}$ than found in *dab1*$^{lacZ/lacZ}$ mice (*dab1*$^{+/+}$ 11±1; *dab1*$^{lacZ/+}$ 11±1; *dab1*$^{lacZ/lacZ}$ 5±1; *dab1*$^{+/+}$ vs *dab1*$^{lacZ/lacZ}$ p=0.003; *dab1*$^{lacZ/+}$ vs *dab1*$^{lacZ/lacZ}$ p=0.004; Villeda *et al.*, 2006; Akopians *et al.*, 2008). Here we report that almost 70% of the Dab1 neurons in the LSN co-express Lmx1b (Fig. 5B, yellow arrowheads in Fig. 5D, D1-2, F, F1-2), with almost twice as many Dab1-Lmx1b neurons in *Reln*$^{+/+}$ (3.2±0.5) than *Reln*$^{-/-}$ LSN (1.7±0.2; p=0.008, Fig. 5H). The total Dab1-positive neurons in *Reln*$^{+/+}$ (5±1) is also greater than in *Reln*$^{-/-}$ LSN (3±0.3; p=0.02, Fig. 5H). Thus Dab1 cells from the lateral reticulated area and the LSN are incorrectly positioned in *Reln*$^{-/-}$ mice, including those that co-localize with Lmx1b.

Dab1-Lmx1b-positive neurons participate in nociceptive circuits

Having determined that the majority of the Dab1-expressing neurons in the superficial dorsal horn, lateral reticulated area, and LSN co-express Lmx1b, we next asked if the Dab1-Lmx1b neurons are activated by noxious thermal or mechanical stimulation. We found clear examples of Fos protein expression in Dab1-Lmx1b-positive neurons in *dab1*$^{+/+}$ and *Reln*$^{+/+}$ superficial dorsal horn (Fig. 6A, A1-4, C, C1-4). Triple-labeled cells (white arrowheads) in the wild-type lateral reticulated area (Fig. 6B, B1-4, D, D1-4) also were detected after thermal or mechanical stimulation. Dab1-Fos- (magenta arrows) and Lmx1b-Fos- (cyan arrows) expressing neurons also were evident (colored arrows in Fig. 6A, A1-3, B, B1-3, C, C1-3, D, D1-3). Thus Dab1-, Lmx1b-, and Dab1-Lmx1b neurons participate in both noxious heat and mechanical circuits.

Lateral cervical nucleus: Dab1 neurons sustain positioning errors in Reelin-signaling pathway mutants

The neurons of the lateral cervical nucleus (LCN; Fig. 7A) are surrounded by axons of the dorsolateral funiculus, but only in cervical levels 1–3 (Kajander and Giesler, 1987). The areas of LCN and LSN cannot be differentiated in these upper cervical levels and thus are analyzed together (Burstein *et al.*, 1990). The LCN neurons receive nociceptive information from neurons throughout the spinal cord and convey it rostrally as part of the spinocervicothalamic pathway (Giesler *et al.*, 1979; Kajander and Giesler, 1987; Burstein *et al.*, 1990). Most LCN neurons project to contralateral thalamus and respond to a wide-range of innocuous and noxious thermal and mechanical stimuli (Giesler *et al.*, 1979; Kajander and Giesler, 1987).

Due to the importance of this area in relaying nociceptive information, we first examined the LCN to determine if neuronal mispositioning in this region might contribute to the sensory abnormalities in Reelin pathway mutants. The Dab1 expression in the C1-3 segments had strong immunoreactivity in neurons of laminae I–II and in the combined LCN/LSN (Fig. 7B–D). The *dab1*$^{lacZ/+}$ LCN/LSN contains neurons that are double-labeled with β-gal and Dab1 (brown, Fig. 7E), whereas the *dab1*$^{lacZ/lacZ}$ has only β-gal concentrated in laminae I–II, the lateral reticulated area, and in the LCN/LSN area (Fig. 7F). This demonstrates that the pattern of Dab1 expression at high cervical levels resembles that in lumbar spinal cord (Fig. 2).

We next asked if LCN neurons are mispositioned in *dab1*$^{lacZ/lacZ}$ mice. The *dab1*$^{+/+}$ LCN/LSN contained an average of 90±6 neurons/dorsal horn and did not differ from *dab1*$^{lacZ/+}$ LCN/LSN with 87±5 neurons. The *dab1*$^{lacZ/lacZ}$ LCN/LSN contained 46±2 NeuN-labeled neurons, 49% and 47% fewer neurons than in *dab1*$^{+/+}$ and *dab1*$^{lacZ/+}$ mice, respectively (*dab1*$^{+/+}$ vs *dab1*$^{lacZ/lacZ}$ p=0.00002; *dab1*$^{lacZ/+}$ vs *dab1*$^{lacZ/lacZ}$ p=0.00004; Fig. 7G–I). We also analyzed *Reln*$^{+/+}$ and *Reln*$^{-/-}$ LCN/LSN neurons and found that on average, *Reln*$^{+/+}$ LCN/LSN contained 78±7 neurons/dorsal horn while *Reln*$^{-/-}$ mice had 41±5 neurons, a 48% reduction in LCN/LSN neurons (p=0.007). Interestingly, nearly 50% of both *dab1*$^{lacZ/lacZ}$ and *Reln*$^{-/-}$ LCN/LSN neurons are displaced, findings which support our contention that this disruption is due to the loss of the canonical Reelin-Dab1 signaling pathway.

The LCN/LSN contains fewer Dab1-Lmx1b neurons and is compressed in Reelin-signaling pathway mutants

Previously we reported that the LSN contained many NK-1R-labeled processes (Akopians *et al.*, 2008). Therefore, to further analyze the LCN/LSN, we estimated the width of this region by measuring the distribution of NK-1R expression in *dab1*^{lacZ} and *Reln* C1-3 segments. NK-1R expression in the LCN/LSN area was measured from the base of the dorsal horn to the most ventral processes that express NK-1R. This distance was greater in the *dab1*$^{+/+}$ (146±6 μm) and *dab1*$^{lacZ/+}$ (140±5 μm) than in *dab1*$^{lacZ/lacZ}$ LCN/LSN (107±0.4 μm; *dab1*$^{+/+}$ vs *dab1*$^{lacZ/lacZ}$ p=0.0005; *dab1*$^{lacZ/+}$vs *dab1*$^{lacZ/lacZ}$ p=0.001; Fig. 7J–L). A similar result was found when comparing the *Reln*$^{+/+}$ and *Reln*$^{-/-}$ LCN/LSN (*Reln*$^{+/+}$ 141±0.7 μm; *Reln*$^{-/-}$ 103±3 μm; p=0.0002). Thus the LCN/LSN in mutants is compacted, consistent with the loss of ~50% of their neurons.

We then analyzed the distribution of Dab1 and Dab1-Lmx1b in ***Reln*** LCN/LSN neurons. On average, both *Reln*$^{+/+}$ and *Reln*$^{-/-}$ LCN/LSN contained 11±1 single-labeled Dab1 neurons, but *Reln*$^{+/+}$ had about twice as many Dab1-Lmx1b neurons as *Reln*$^{-/-}$ LCN/LSN (*Reln*$^{+/+}$ 12±1; *Reln*$^{-/-}$ 6±1; p=0.004; yellow arrowheads in Fig. 8A1-3, B1-3). These results showed that although 52% of Dab1 cells in ***Reln***$^{+/+}$ LCN/LSN co-express Lmx1b, only 36% of Dab1 cells in *Reln*$^{-/-}$ LCN/LSN are double-labeled. Because the LCN/LSN region contains many projection neurons that convey nociceptive signals rostrally, changes in both neuronal density and distribution in Reelin-signaling pathway mutants likely impact the fidelity with which pain messages are transmitted rostrally.

Discussion

To identify anatomical defects in mutants of the Reelin-Dab1 signaling pathway, we first characterized the Dab1-expressing dorsal horn neurons. We found many small Dab1-labeled dorsal horn neurons in laminae I–II and discovered that 70% of these Dab1 interneurons co-expressed the transcription factor Lmx1b. Additionally, areas that contain projection neurons for pain processing, such as the lateral reticulated area, LSN, and the LCN, also contained Dab1 neurons and 50–70% of them co-expressed Lmx1b. Based on previous reports, these neuronal populations are likely to be excitatory glutamatergic neurons (Cheng *et al.*, 2004; Cheng *et al.*, 2005; Dai *et al.*, 2008). Importantly, we found evidence of mispositioned Dab1

neurons in multiple areas of the *Reln*$^{-/-}$ dorsal horn when compared to *Reln*$^{+/+}$: 1) More Dab1 and Dab1-Lmx1b cells are found within the IB4-terminal zone and the IB4 band itself was shifted dorsally, 2) The lateral reticulated area and LSN were missing about 50% of their Dab1-Lmx1b neurons, and 3) The combined LCN/LSN was compressed and missing nearly 50% of its neurons, including many that co-express Dab1-Lmx1b. Additionally, Dab1-Lmx1b neurons in the superficial dorsal horn and lateral reticulated area expressed Fos after thermal and mechanical stimulation and thus actively participated in these nociceptive circuits. Together, we have identified populations of Dab1-expressing dorsal horn interneurons and projection neurons that sustain positioning errors in Reelin-signaling pathway mutants, including a number of glutamatergic neurons. Thus, the thermal hyperalgesia and reduced mechanical sensitivity in *Reln*$^{-/-}$ suggests multiple disruptions in the dorsal horn pain circuits that involve mispositioned Dab1-Lmx1b neurons. These findings highlight the importance of the canonical Reelin-Dab1 signaling pathway in regulating neuronal positioning in dorsal horn nociceptive areas and now correlate anatomical defects with the pain abnormalities observed in mutant mice.

The loss of Reelin in the spinal cord affects Dab1 neurons differently

Both somatic and preganglionic motor neurons in the spinal cord express Dab1 and respond to Reelin signaling, yet in *Reln*$^{-/-}$ and *dab1*$^{-/-}$ mice, somatic motor neurons have rather subtle positioning errors compared to the extensively mispositioned sympathetic and parasympathetic preganglionic neurons (Yip *et al.*, 2000; Phelps *et al.*, 2002; Palmesino *et al.*, 2010; Abadesco *et al.*, 2014). Dab1-labeled dorsal horn neurons also show differences in the extent of their positioning errors. Disruptions in the cellular organization of the smaller Dab1 interneurons in *Reln*$^{-/-}$ laminae I–II were difficult to identify, whereas the larger Dab1 projection neurons in *Reln*$^{-/-}$ lateral reticulated area, LSN, and LCN/LSN were clearly missing from their respective areas. The final locations of these mispositioned Dab1 projection neurons remain unclear but likely include the extra Dab1 and Dab1-Lmx1b neurons in the IB4 area of laminae IIinner and large ectopic cells detected along the outer edge of lamina I.

Based on previous studies, the migratory pathway of Dab1 and the late-born Lmx1b (dIL^{B}) neurons overlap extensively, both temporally and spatially (Müller *et al.*, 2002; Dunston *et al.*, 2005; Villeda *et al.*, 2006; Rebelo *et al.*, 2010). If Reelin functions to terminate the migration of the laterally located Dab1 neurons in the lateral reticulated area, LSN and LCN as reported with the sympathetic preganglionic neurons, then the absence of Reelin would cause these dorsal horn projection neurons to fail to stop laterally and instead migrate past their normal locations or return to the midline (Yip *et al.*, 2000; Phelps *et al.*, 2002; Krüger *et al.*, 2010). On the other hand, the Dab1 neurons in the *Reln*$^{-/-}$ superficial dorsal horn seem to remain near their correct laminae but are somewhat out of place compared to *Reln*$^{+/+}$ mice. Because the number of Dab1 neurons and the percentage of Dab1 neurons co-expressing Lmx1b do not differ between *Reln*$^{+/+}$ and *Reln*$^{-/-}$ superficial dorsal horns, there is no evidence of selective cell death in our model. Furthermore, based on previous studies (Caviness and Rakic, 1978; Rice and Curran, 2001), neuronal generation is usually normal in Reelin-signaling pathway mutants, but their migration pathways are altered.

Dab1 and Lmx1b both identify large neurons in the lateral reticulated area which express Fos following mechanical or thermal stimulation. Based on their size, location, and response to stimulation, these Dab1- and Dab1-Lmx1b cells likely correspond to the so-called wide-dynamic-range neurons that relay nociceptive information to rostral targets (Menétrey *et al.*, 1980). Similarly, Dab1 and Lmx1b also identify large neurons in the LCN/LSN, many of which are likely to be projection neurons that relay nociceptive information to the thalamus (Giesler *et al.*, 1979; Kajander and Giesler, 1987). The significant positioning errors sustained by these neurons imply that Reelin regulates their migration during development. Although generally the correct afferents still contact mispositioned neurons, it is unclear whether or not normal functional connections are formed (Yip *et al.*, 2003; Pascual *et al.*, 2004), especially since Reelin signaling was found to play a role in regulating hippocampal synaptic function (Qiu *et al.*, 2006; Pujadas *et al.*, 2010). In addition, Reelin-Dab1 signaling has been implicated in dendrite development in the hippocampus and the cerebral cortex (Niu *et al.*, 2004; Olson *et al.*, 2006; Matsuki *et al.*, 2008). ***Reln*$^{-/-}$ and *dab1*$^{-/-}$** somatic motor neurons also have stunted dendrites compared to wild-type mice (Phelps *et al.*, 2002; Abadesco *et al.*, 2014). Thus without Reelin, the Dab1 dorsal horn neurons also may have abnormal dendrites, in addition to being mispositioned, which would further impair their neuronal connections.

The contributions of Reelin and Lmx1b to nociception

Three recent mutant mouse studies (Wang *et al.*, 2013; Xu *et al.*, 2013; Szabo *et al.*, 2015) that characterized excitatory interneurons in the superficial dorsal horn found elevated withdrawal thresholds in response to mechanical stimulation and morphological alterations that resemble the phenotypic changes reported in our study. Furthermore, the brain-sparing deletion of *Lmx1b* (Szabo *et al.*, 2015), the removal of *Tlx3* from the excitatory dI5 and dIL^{B} neurons (Xu *et al.*, 2013), and the CNS-specific deletion of *TR4*, a testicular orphan nuclear receptor (Wang *et al.*, 2013), all reported changes in the lamination pattern of the superficial dorsal horn and a loss in the number of laminae I–II neurons. Of particular interest to our study was the loss of about 70% of Reelin-labeled superficial dorsal horn cells in both *TR4* and *Lmx1b* mutant mice (Wang *et al.*, 2013; Szabo *et al.*, 2015). The absence of Reelin-expressing cells in the superficial dorsal horn would likely impact Dab1-expressing cells severely.

Although Reelin-signaling pathway mutants are relatively insensitive to mechanical stimulation as are the *TR4* and *Lmx1b* conditional knockout mice, it is interesting that *Reln*$^{-/-}$ and *dab1*$^{-/-}$ mice have the opposite response to heat, i.e., thermal hyperalgesia (Villeda *et al.*, 2006; Akopians *et al.*, 2008; Wang *et al.*, 2012). Thus there must be a different neural circuit involving the Reelin-signaling pathway by which heat sensitivity is increased. These findings imply that the canonical Reelin pathway differentially affects circuits that process noxious thermal heat and mechanical signals and adds further support to the concept of modality-specific circuits that process painful heat and mechanical messages.

Acknowledgments

We thank Dr. Allan Basbaum for valuable guidance and suggestions on the manuscript, Dr. Brian Howell for providing the *dab1*^{lacZ} mice and Dab1 antibody, Drs. Carmen Birchmeier and Thomas Müller for providing Lmx1b

antibody, Dr. Alin Akopians for helpful comments on the manuscript, Frank Lee for assistance with *Reln*$^{rl–Orl;}$ *GAD67*^{GFP} data, and Aly Mulji for mouse colony care and completing the NK-1R data analyses. This study acknowledges support from the National Science Foundation (IOB-0924143 to PEP) and the Microscopy Core of the IDDRC from the NICHD (P30HD004612 and U54HD087101).

Abbreviations

ChAT	choline acetyltransferase
CNS	central nervous system
Dab1	disabled-1
GAD67	glutamic acid decarboxylase 67
GFP	green fluorescent protein
IB4	isolectin B4
LCN	lateral cervical nucleus
Lmx1b	LIM-homeobox transcription factor 1 beta
LSN	lateral spinal nucleus
NeuN	neuronal nuclei
NK-1R	neurokinin-1 receptor
PB	phosphate buffer
PKCγ	protein kinase C gamma
Tlx3	T-cell leukemia homeobox 3
TR4	testicular orphan nuclear receptor 4

References

Abadesco AD, Cilluffo M, Yvone GM, Carpenter EM, Howell BW, Phelps PE. Novel Disabled-1-expressing neurons identified in adult brain and spinal cord. Eur J Neurosci. 2014; 39:579–592. [PubMed: 24251407]

Akopians AL, Babayan AH, Beffert U, Herz J, Basbaum AI, Phelps PE. Contribution of the Reelin signaling pathways to nociceptive processing. Eur J Neurosci. 2008; 27:523–537. [PubMed: 18279306]

Antal M, Polgár E, Chalmers J, Minson JB, Llewellyn-Smith I, Heizmann CW, Somogyi P. Different populations of parvalbumin- and calbindin-D28k-immunoreactive neurons contain GABA and accumulate ^{3}H-D-aspartate in the dorsal horn of the rat spinal cord. J Comp Neurol. 1991; 314:114–124. [PubMed: 1797867]

Arnaud L, Ballif BA, Cooper JA. Regulation of protein tyrosine kinase signaling by substrate degradation during brain development. Mol Cell Biol. 2003; 23:9293–9302. [PubMed: 14645539]

Basbaum AI, Bautista DM, Scherrer G, Julius D. Cellular and molecular mechanisms of pain. Cell. 2009; 139:267–284. [PubMed: 19837031]

Bock HH, Herz J. Reelin activates SRC family tyrosine kinases in neurons. Curr Biol. 2003; 13:18–26. [PubMed: 12526740]

Burstein R, Cliffer KD, Giesler GJ Jr. Direct somatosensory projections from the spinal cord to the hypothalamus and telencephelon. J Neurosci. 1987; 7:4159–4164. [PubMed: 3694268]

Burstein R, Dado RJ, Giesler GJ Jr. The cells of origin of the spinothalamic tract of the rat: a quantitative reexamination. Brain Res. 1990; 511:329–337. [PubMed: 2334851]

Caviness VS Jr, Rakic P. Mechanisms of cortical development: a view from mutations in mice. Annu Rev Neurosci. 1978; 1:297–326. [PubMed: 386903]

Chaplan SR, Bach FW, Pogrel JW, Chung JM, Yaksh TL. Quantitative assessment of tactile allodynia in the rat paw. J Neurosci Methods. 1994; 53:55–63. [PubMed: 7990513]

Cheng L, Arata A, Mizuguchi R, Qian Y, Karunaratne A, Gray PA, Arata S, Shirasawa S, Bouchard M, Luo P, Chen CL, Busslinger M, Goulding M, Onimaru H, Ma Q. Tlx3 and Tlx1 are post-mitotic selector genes determining glutamatergic over GABAergic cell fates. Nat Neurosci. 2004; 7:510–517. [PubMed: 15064766]

Cheng L, Samad OA, Xu Y, Mizuguchi R, Luo P, Shirasawa S, Goulding M, Ma Q. Lbx1 and Tlx3 are opposing switches in determining GABAergic versus glutamatergic transmitter phenotypes. Nat Neurosci. 2005; 8:1510–1515. [PubMed: 16234809]

D'Arcangelo G, Miao GG, Curran T. Detection of the reelin breakpoint in reeler mice. Brain Res Mol Brain Res. 1996; 39:234–236. [PubMed: 8804731]

Dai JX, Hu ZL, Shi M, Guo C, Ding YQ. Postnatal ontogeny of the transcription factor Lmx1b in the mouse central nervous system. J Comp Neurol. 2008; 509:341–355. [PubMed: 18512225]

Dunston JA, Reimschisel T, Ding YQ, Sweeney E, Johnson RL, Chen ZF, McIntosh I. A neurological phenotype in nail patella syndrome (NPS) patients illuminated by studies of murine Lmx1b expression. Eur J Hum Genet. 2005; 13:330–335. [PubMed: 15562281]

Giesler GJ Jr, Urca G, Cannon JT, Liebeskind JC. Response properties of neurons of the lateral cervical nucleus in the rat. J Comp Neurol. 1979; 186:65–77. [PubMed: 457931]

Gross MK, Dottori M, Goulding M. Lbx1 specifies somatosensory association interneurons in the dorsal spinal cord. Neuron. 2002; 34:535–549. [PubMed: 12062038]

Gutierrez-Mecinas M, Furuta T, Watanabe M, Todd AJ. A quantitative study of neurochemically defined excitatory interneuron populations in laminae I–III of the mouse spinal cord. Mol Pain. 2016; 12 pii: 1744806916629065.

Hammond V, So E, Gunnersen J, Valcanis H, Kalloniatis M, Tan SS. Layer positioning of late-born cortical interneurons is dependent on Reelin but not p35 signaling. J Neurosci. 2006; 26:1646–1655. [PubMed: 16452688]

Hargreaves K, Dubner R, Brown F, Flores C, Joris J. A new and sensitive method for measuring thermal nociception in cutaneous hyperalgesia. Pain. 1988; 32:77–88. [PubMed: 3340425]

Honda T, Kobayashi K, Mikoshiba K, Nakajima K. Regulation of cortical neuron migration by the Reelin signaling pathway. Neurochem Res. 2011; 36:1270–1279. [PubMed: 21253854]

Howell BW, Hawkes R, Soriano P, Cooper JA. Neuronal position in the developing brain is regulated by mouse disabled-1. Nature. 1997; 389:733–737. [PubMed: 9338785]

Kajander KC, Giesler GJ Jr. Responses of neurons in the lateral cervical nucleus of the cat to noxious cutaneous stimulation. J Neurophysiol. 1987; 57:1686–1704. [PubMed: 3598627]

Kayalioglu G, Robertson B, Kristensson K, Grant G. Nitric oxide synthase and interferon-gamma receptor immunoreactivities in relation to ascending spinal pathways to thalamus, hypothalamus, and the periaqueductal grey in the rat. Somatosens Mot Res. 1999; 16:280–290. [PubMed: 10632025]

Krüger MT, Zhao S, Chai X, Brunne B, Bouché E, Bock HH, Frotscher M. Role for Reelin-induced cofilin phosphorylation in the assembly of sympathetic preganglionic neurons in the murine intermediolateral column. Eur J Neurosci. 2010; 32:1611–1617. [PubMed: 21039973]

Kubasak MD, Brooks R, Chen S, Villeda SA, Phelps PE. Developmental distribution of reelin-positive cells and their secreted product in the rodent spinal cord. J Comp Neurol. 2004; 468:165–178. [PubMed: 14648677]

Laing I, Todd AJ, Heizmann CW, Schmidt HH. Subpopulations of GABAergic neurons in laminae I–III of rat spinal dorsal horn defined by coexistence with classical transmitters, peptides, nitric oxide synthase or parvalbumin. Neuroscience. 1994; 61:123–132. [PubMed: 7526265]

Matsuki T, Pramatarova A, Howell BW. Reduction of Crk and CrkL expression blocks reelin-induced dendritogenesis. J Cell Sci. 2008; 121:1869–1875. [PubMed: 18477607]

Menétrey D, Chaouch A, Besson JM. Location and properties of dorsal horn neurons at origin of spinoreticular tract in lumbar enlargement of the rat. J Neurophysiol. 1980; 44:862–877. [PubMed: 7441321]

Menétrey D, Chaouch A, Binder D, Besson JM. The origin of the spinomesencephalic tract in the rat: an anatomical study using the retrograde transport of horseradish peroxidase. J Comp Neurol. 1982; 206:193–207. [PubMed: 7085928]

Müller T, Brohmann H, Pierani A, Heppenstall PA, Lewin GR, Jessell TM, Birchmeier C. The homeodomain factor Lbx1 distinguishes two major programs of neuronal differentiation in the dorsal spinal cord. Neuron. 2002; 34:551–562. [PubMed: 12062039]

Niu S, Renfro A, Quattrocchi CC, Sheldon M, D'Arcangelo G. Reelin promotes hippocampal dendrite development through the VLDLR/ApoER2-Dab1 pathway. Neuron. 2004; 41:71–84. [PubMed: 14715136]

Olson EC, Kim S, Walsh CA. Impaired neuronal positioning and dendritogenesis in the neocortex after cell-autonomous Dab1 suppression. J Neurosci. 2006; 26:1767–1775. [PubMed: 16467525]

Palmesino E, Rousso DL, Kao TJ, Klar A, Laufer E, Uemura O, Okamoto H, Novitch BG, Kania A. Foxp1 and lhx1 coordinate motor neuron migration with axon trajectory choice by gating Reelin signaling. PLoS Biol. 2010; 8:e1000446. [PubMed: 20711475]

Pascual M, Pérez-Sust P, Soriano E. The GABAergic septohippocampal pathway in control and reeler mice: target specificity and termination onto Reelin-expressing interneurons. Mol Cell Neurosci. 2004; 25:679–691. [PubMed: 15080896]

Phelps PE, Barber RP, Houser CR, Crawford GD, Salvaterra PM, Vaughn JE. Postnatal development of neurons containing choline acetyltransferase in rat spinal cord: an immunocytochemical study. J Comp Neurol. 1984; 229:347–361. [PubMed: 6389614]

Phelps PE, Rich R, Dupuy-Davies S, Ríos Y, Wong T. Evidence for a cell-specific action of Reelin in the spinal cord. Dev Biol. 2002; 244:180–198. [PubMed: 11900467]

Pramatarova A, Chen K, Howell BW. A genetic interaction between the APP and Dab1 genes influences brain development. Mol Cell Neurosci. 2008; 37:178–186. [PubMed: 18029196]

Pujadas L, Gruart A, Bosch C, Delgado L, Teixeira CM, Rossi D, de Lecea L, Martínez A, Delgado-García JM, Soriano E. Reelin regulates postnatal neurogenesis and enhances spine hypertrophy and long-term potentiation. J Neurosci. 2010; 30:4636–4649. [PubMed: 20357114]

Qiu S, Korwek KM, Pratt-Davis AR, Peters M, Bergman MY, Weeber EJ. Cognitive disruption and altered hippocampus synaptic function in Reelin haploinsufficient mice. Neurobiol Learn Mem. 2006; 85:228–242. [PubMed: 16376115]

Rebelo S, Reguenga C, Lopes C, Lima D. Prrxl1 is required for the generation of a subset of nociceptive glutamatergic superficial spinal dorsal horn neurons. Dev Dyn. 2010; 239:1684–1694. [PubMed: 20503365]

Rice DS, Sheldon M, D'Arcangelo G, Nakajima K, Goldowitz D, Curran T. Disabled-1 acts downstream of Reelin in a signaling pathway that controls laminar organization in the mammalian brain. Development. 1998; 125:3719–3729. [PubMed: 9716537]

Rice DS, Curran T. Role of the reelin signaling pathway in central nervous system development. Annu Rev Neurosci. 2001; 24:1005–1039. [PubMed: 11520926]

Shields SD, Moore KD, Phelps PE, Basbaum AI. Olfactory ensheathing glia express Aquaporin 1. J Comp Neurol. 2010; 518:4329–4341. [PubMed: 20853510]

Szabo NE, da Silva RV, Sotocinal SG, Zeilhofer HU, Mogil JS, Kania A. Hoxb8 intersection defines a role for Lmx1b in excitatory dorsal horn neuron development, spinofugal connectivity, and nociception. J Neurosci. 2015; 35:5233–5246. [PubMed: 25834049]

Takahara T, Ohsumi T, Kuromitsu J, Shibata K, Sasaki N, Okazaki Y, Shibata H, Sato S, Yoshiki A, Kusakabe M, Muramatsu M, Ueki M, Okuda K, Hayashizaki Y. Dysfunction of the Orleans reeler gene arising from exon skipping due to transposition of a full-length copy of an active L1 sequence into the skipped exon. Hum Mol Genet. 1996; 5:989–993. [PubMed: 8817336]

Tamamaki N, Yanagawa Y, Tomioka R, Miyazaki J, Obata K, Kaneko T. Green fluorescent protein expression and colocalization with calretinin, parvalbumin, and somatostatin in the GAD67-GFP knock-in mouse. J Comp Neurol. 2003; 467:60–79. [PubMed: 14574680]

Todd AJ. Neuronal circuitry for pain processing in the dorsal horn. Nat Rev Neurosci. 2010; 11:823–836. [PubMed: 21068766]

Trommsdorff M, Gotthardt M, Hiesberger T, Shelton J, Stockinger W, Nimpf J, Hammer RE, Richardson JA, Herz J. Reeler/Disabled-like disruption of neuronal migration in knockout mice lacking the VLDL receptor and ApoE receptor 2. Cell. 1999; 97:689–701. [PubMed: 10380922]

Villeda SA, Akopians AL, Babayan AH, Basbaum AI, Phelps PE. Absence of Reelin results in altered nociception and aberrant neuronal positioning in the dorsal spinal cord. Neuroscience. 2006; 139:1385–1396. [PubMed: 16580148]

Wang X, Babayan AH, Basbaum AI, Phelps PE. Loss of the Reelin-signaling pathway differentially disrupts heat, mechanical and chemical nociceptive processing. Neuroscience. 2012; 226:441–450. [PubMed: 22999972]

Wang X, Zhang J, Eberhart D, Urban R, Meda K, Solorzano C, Yamanaka H, Rice D, Basbaum AI. Excitatory superficial dorsal horn interneurons are functionally heterogeneous and required for the full behavioral expression of pain and itch. Neuron. 2013; 78:312–324. [PubMed: 23622066]

Xu Y, Lopes C, Wende H, Guo Z, Cheng L, Birchmeier C, Ma Q. Ontogeny of excitatory spinal neurons processing distinct somatic sensory modalities. J Neurosci. 2013; 33:14738–14748. [PubMed: 24027274]

Yip JW, Yip YP, Nakajima K, Capriotti C. Reelin controls position of autonomic neurons in the spinal cord. Proc Natl Acad Sci U S A. 2000; 97:8612–8616. [PubMed: 10880573]

Yip YP, Rinaman L, Capriotti C, Yip JW. Ectopic sympathetic preganglionic neurons maintain proper connectivity in the reeler mutant mouse. Neuroscience. 2003; 118:439–50. [PubMed: 12699780]

Yip YP, Capriotti C, Magdaleno S, Benhayon D, Curran T, Nakajima K, Yip JW. Components of the reelin signaling pathway are expressed in the spinal cord. J Comp Neurol. 2004; 470:210–219. [PubMed: 14750162]

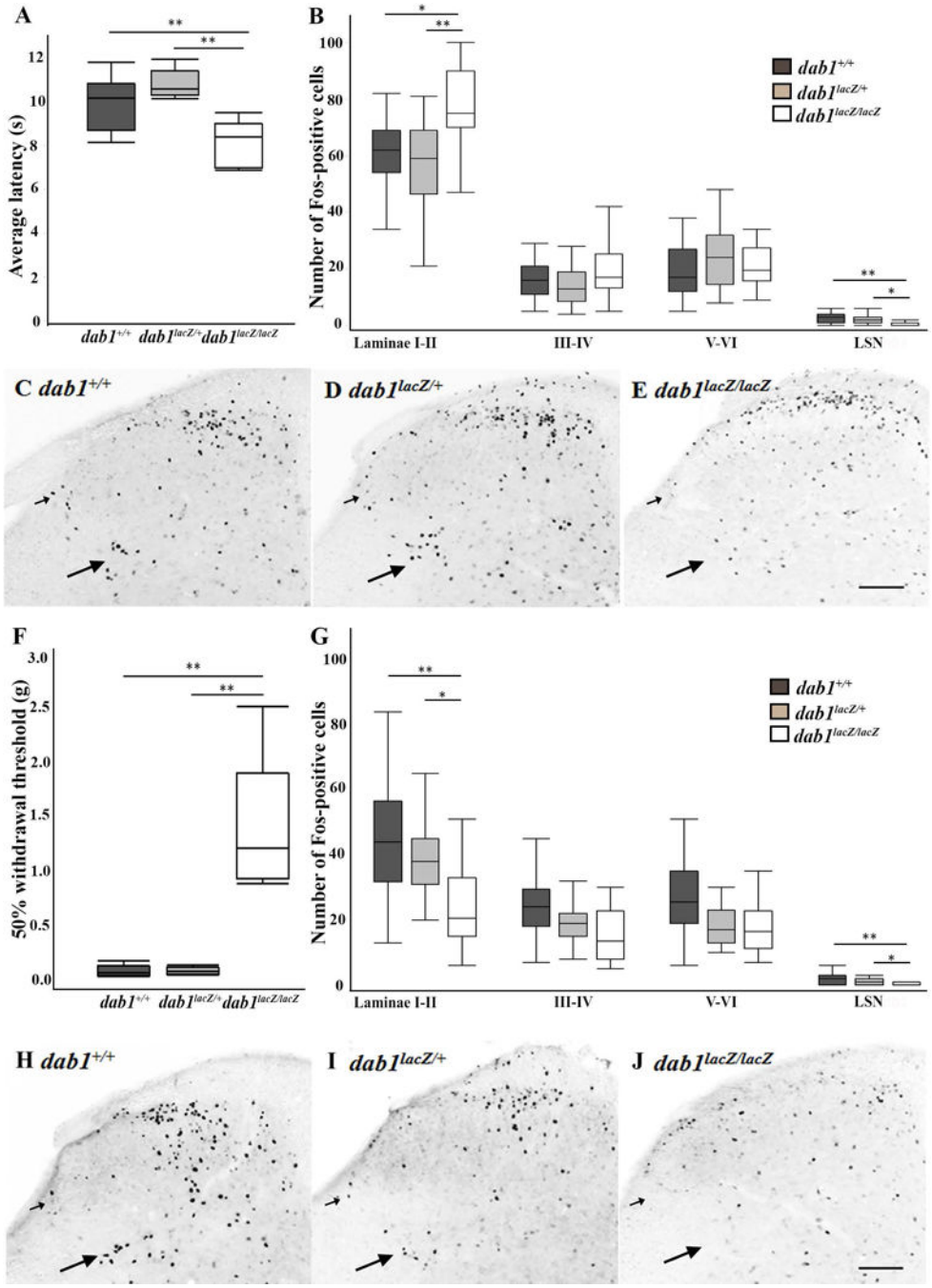

Figure 1. *dab1*$^{lacZ/lacZ}$ mice are hypersensitive to thermal and have reduced sensitivity to mechanical stimulation

A, Thermal sensitivity measured by the Hargreaves test. The mean latency±SEM for *dab1*$^{+/+}$ is 9.9±0.5s, for *dab1*$^{lacZ/+}$ is 10.8±0.3s, and for *dab1*$^{lacZ/lacZ}$ is 8.2±0.4s. There are significant differences between *dab1*$^{+/+}$ vs *dab1*$^{lacZ/lacZ}$ (p=0.01) and for *dab1*$^{lacZ/+}$ vs *dab1*$^{lacZ/lacZ}$ (p=0.0005). ***B***, After heat stimulation, there are on average fewer Fos-positive neurons in *dab1*$^{+/+}$ (60.5±2.9 neurons) and *dab1*$^{lacZ/+}$ (55.6±6) than in *dab1*$^{lacZ/lacZ}$ (75.9±3.9) laminae I–II (*dab1*$^{+/+}$vs *dab1*$^{lacZ/lacZ}$ p=0.047; *dab1*$^{lacZ/+}$vs *dab1*$^{lacZ/lacZ}$ p=0.01).

More Fos-positive neurons were present in the lateral spinal nucleus (LSN) of *dab1*$^{+/+}$ (2.6±0.4) and *dab1*$^{lacZ/+}$ (2.1±0.5) than in *dab1*$^{lacZ/lacZ}$ mice (0.6±0.1; *dab1*$^{+/+}$vs *dab1*$^{lacZ/lacZ}$ p=0.004; *dab1*$^{lacZ/+}$vs *dab1*$^{lacZ/lacZ}$ p=0.02). ***C–E***, After heat stimulation, there are fewer Fos-labeled neurons in laminae I–II but more in the lateral reticulated area of lamina V (long arrows) and LSN (short arrows) of *dab1*$^{+/+}$ and *dab1*$^{lacZ/+}$ than in *dab1*$^{lacZ/lacZ}$ mice (medial to the right in coronal sections of all figures). ***F***, The von Frey test of mechanical sensitivity found that the withdrawal thresholds from *dab1*$^{+/+}$ (0.07±0.02g) and *dab1*$^{lacZ/+}$ (0.07±0.01g) mice do not differ, whereas *dab1*$^{lacZ/lacZ}$ responses are profoundly slower (1.37±0.3g; *dab1*$^{+/+}$vs *dab1*$^{lacZ/lacZ}$ p=0.004; *dab1*$^{lacZ/+}$vs *dab1*$^{lacZ/lacZ}$ p=0.004). ***G***, After mechanical stimulation, more Fos-positive neurons are in *dab1*$^{+/+}$ (43.8±5) and *dab1*$^{lacZ/+}$ (39.2±1.8) compared with *dab1*$^{lacZ/lacZ}$ laminae I–II (24.5±5; *dab1*$^{+/+}$vs *dab1*$^{lacZ/lacZ}$ p=0.005; *dab1*$^{lacZ/+}$vs *dab1*$^{lacZ/lacZ}$ p=0.03) and in *dab1*$^{+/+}$ (1.8±0.4) and *dab1*$^{lacZ/+}$ (1.3±0.1) than *dab1*$^{lacZ/lacZ}$ LSN (0.4±0.2; *dab1*$^{+/+}$vs *dab1*$^{lacZ/lacZ}$ p=0.004; *dab1*$^{lacZ/+}$vs *dab1*$^{lacZ/lacZ}$ p=0.047). ***H–J***, More Fos-expressing cells appear in *dab1*$^{+/+}$ and *dab1*$^{lacZ/+}$ laminae I–II, lateral reticulated area (long arrows), and LSN (short arrows) than in *dab1*$^{lacZ/lacZ}$ mice. Scale bars: ***C–E***; ***H–J***, 200 μm.

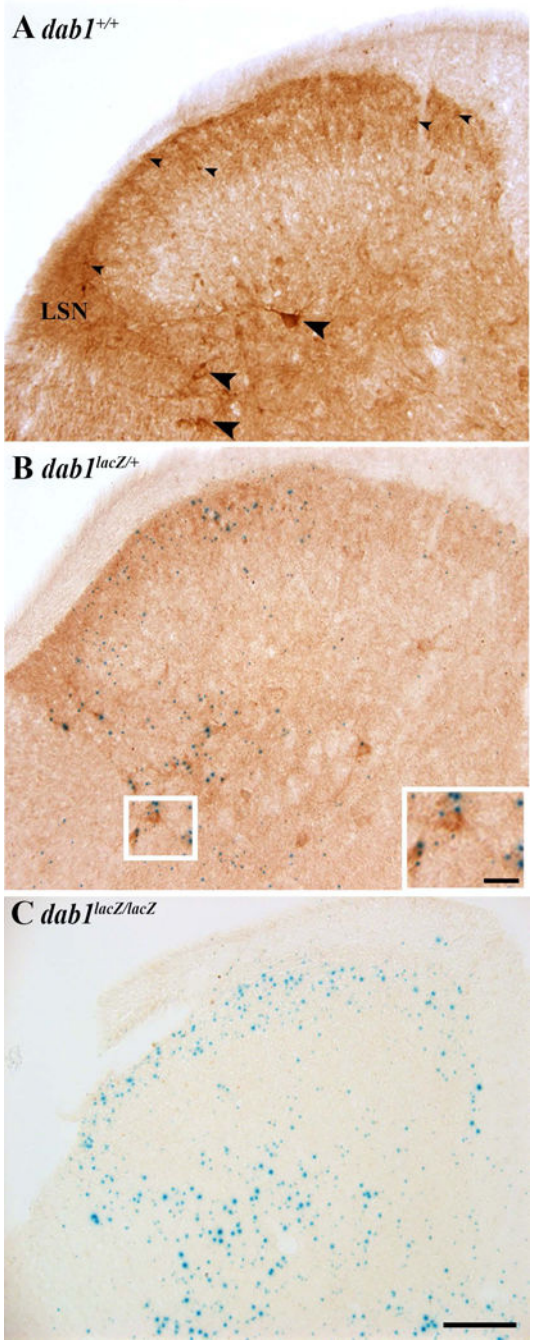

Figure 2. Dab1 and β-galactosidase are co-expressed in the dorsal horn

A, Dab1 immunoreactivity (brown) concentrated in *dab1*$^{+/+}$ laminae I–II, lateral reticulated area of lamina V, and the lateral spinal nucleus (LSN). Relatively small Dab1 neurons (small arrowheads) are in laminae I–II whereas medium and large Dab1 neurons (large arrowheads) are found in the lateral reticulated area. ***B***, The *dab1*$^{lacZ/+}$ dorsal horn contains both brown Dab1 and blue β-gal precipitate. The colocalization seen in the boxed lateral reticulated area is enlarged in the inset. ***C***, The *dab1*$^{lacZ/lacZ}$ dorsal horn contains a pattern of blue β-gal

reaction product similar to Dab1 immunoreactivity shown in A and B. Scale bar: ***A–C***, 200 μm; **Inset in *B*, 50 μm.**

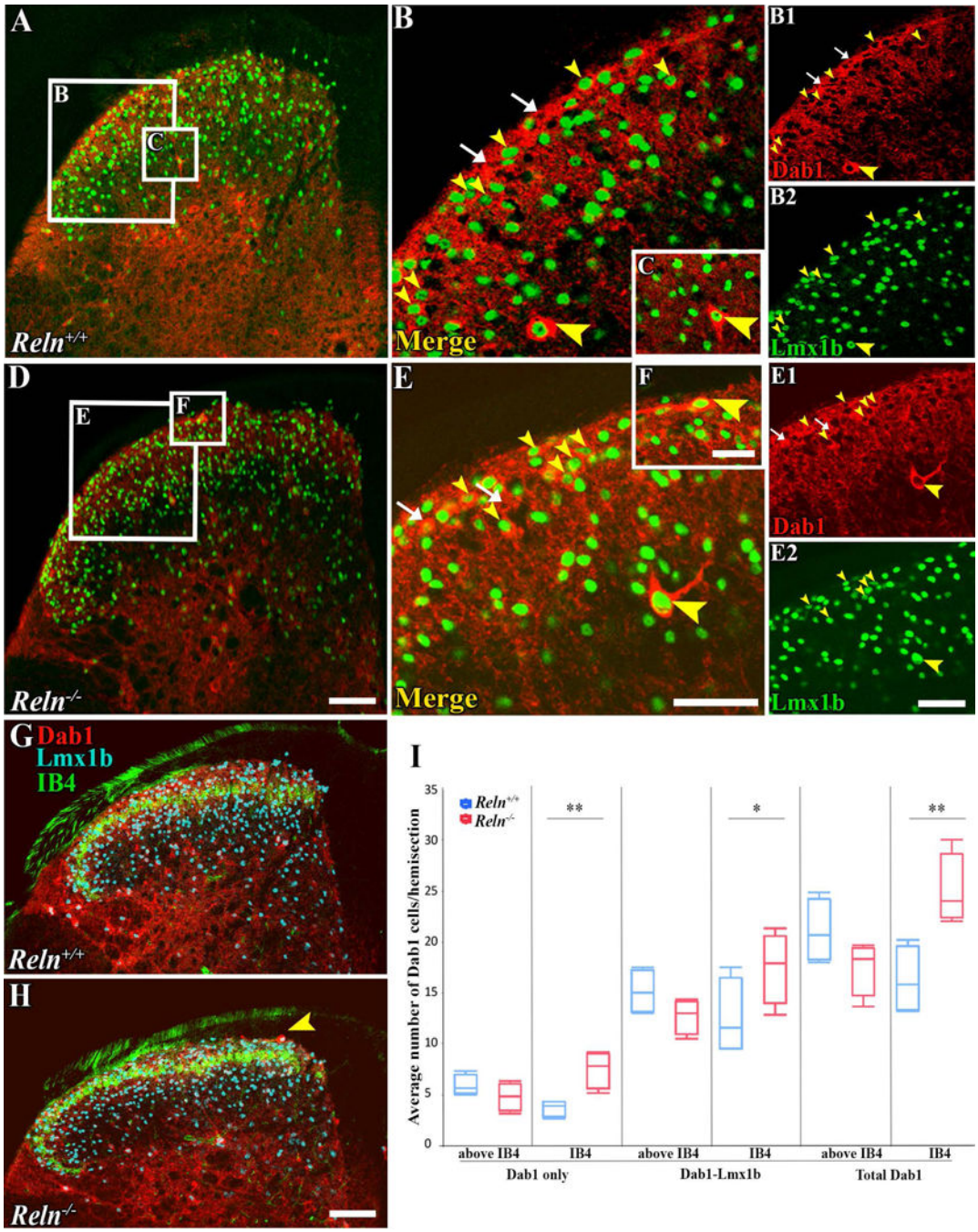

Figure 3. Superficial dorsal horn: 70% of Dab1 cells co-express Lmx1b and are mispositioned within the *Reln*$^{-/-}$ IB4 terminal zone

A–F, Confocal 3 μm thick images of *Reln*$^{+/+}$ (***A–C***) and *Reln*$^{-/-}$ (***D–F***) lumbar dorsal horns show that many cells express both Dab1 (red cytoplasm) and Lmx1b (green nucleus), including small interneurons in laminae I–II (small yellow arrowheads) and large neurons in laminae I–III (large yellow arrowheads). Examples of single-labeled Dab1 cells are marked by white arrows. Boxes in ***A*** and ***D*** are enlarged in ***B***, ***C***, ***E***, and ***F***. Individual channels of ***B*** and ***E*** are labeled ***B1-2*** and ***E1-2***. ***G–H***, Lumbar confocal images show the distribution of

Dab1 (red) and Lmx1b (cyan) within and above the IB4 (green) band of terminals. Although the area of lamina II marked by IB4 afferents does not vary by genotype, the area of laminae I–IIouter, located dorsal to the IB4 terminals, is larger in *Reln*$^{+/+}$ than in *Reln*$^{-/-}$ mice. An arrowhead marks a large ectopic Dab1-Lmx1b neuron in *Reln*$^{-/-}$ lamina I. ***I***, The number of Dab1 cells in laminae I–II outer, i.e., above the IB4 area, do not vary by genotype, but more Dab1, Dab1-Lmx1b, and total Dab1 neurons are found within the *Reln*$^{-/-}$ compared to the *Reln*$^{+/+}$ IB4 band (n=4 mice/genotype). Scale bars: ***A***, ***D***; ***G–H***, 100 μm; ***B***, ***E***; ***C***, ***F***; ***B1-2***, ***E1-2***, 50 μm.

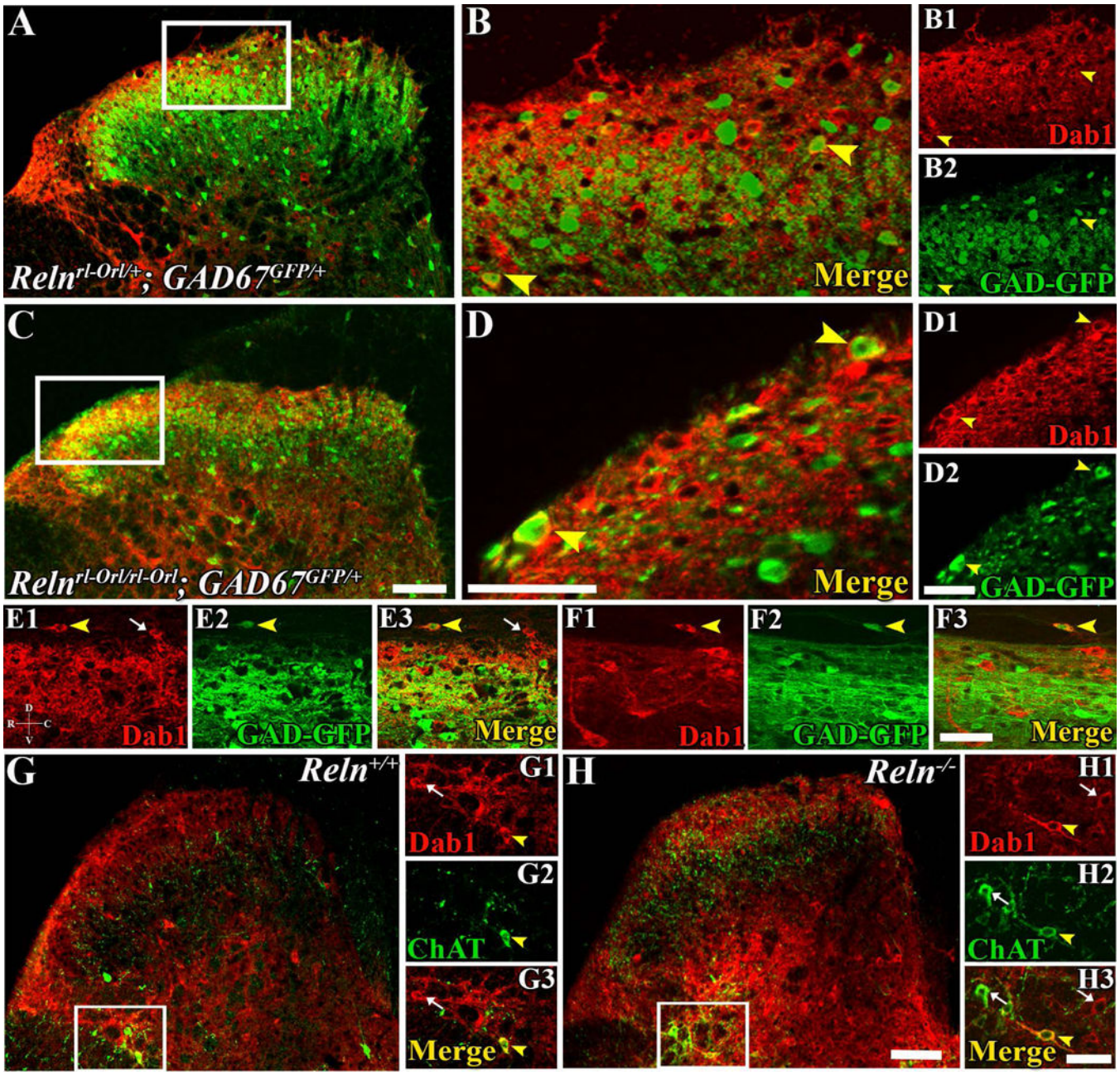

Figure 4. A small number of Dab1 neurons in laminae I–II are GABAergic and in the lateral reticulated area are cholinergic

A–D, Confocal images of *Reln*$^{rl-Orl/+}$*; GAD67*$^{GFP/+}$ (***A–B***) and *Reln*$^{rl-Orl/rl-Orl}$*; GAD67*$^{GFP/+}$ (***C–D***) lumbar dorsal horns. Boxes in ***A*** and ***C*** are enlarged in ***B*** and ***D***, with individual channels in ***B1-2*** and ***D1-2***. A few Dab1 (red) and GAD67^{GFP} neurons appear co-localized (yellow arrowheads in ***B*** and ***D***). ***E–F***, Sagittal lumbar dorsal horn sections from *Reln-Orl*$^{+/+}$*;GAD67*$^{GFP/+}$ (***E1-3***) and *Reln*$^{rl-Orl/rl-Orl}$*; GAD67*$^{GFP/+}$ (***F1-3***) mice illustrate ectopic cells in the white matter dorsal to lamina I. Dab1 (white arrows in ***E1***, ***3***) and Dab1-GAD67^{GFP}-labeled (yellow arrowheads in ***E1-3***, ***F1-3***) neurons are frequently found dorsal to lamina I (top of image). ***G–H***, *Reln*$^{+/+}$ and *Reln*$^{-/-}$ dorsal horns show that Dab1 (red) and

ChAT-positive neurons (green) do not co-localize in laminae I–IV, but double-labeled cells boxed in ***G*** and ***H*** (yellow arrowheads in ***G1-3***, ***H1-3***) are found in the lateral reticulated area of lamina V. Single-labeled Dab1 and ChAT neurons are marked with white arrows. Scale bars: ***A***, ***C***; ***G–H***, 100 μm; ***B***, ***D***; ***B1-2***, ***D1-2***; ***E1-3***, ***F1-3***; ***G1-3***, ***H1-3***, 50 μm.

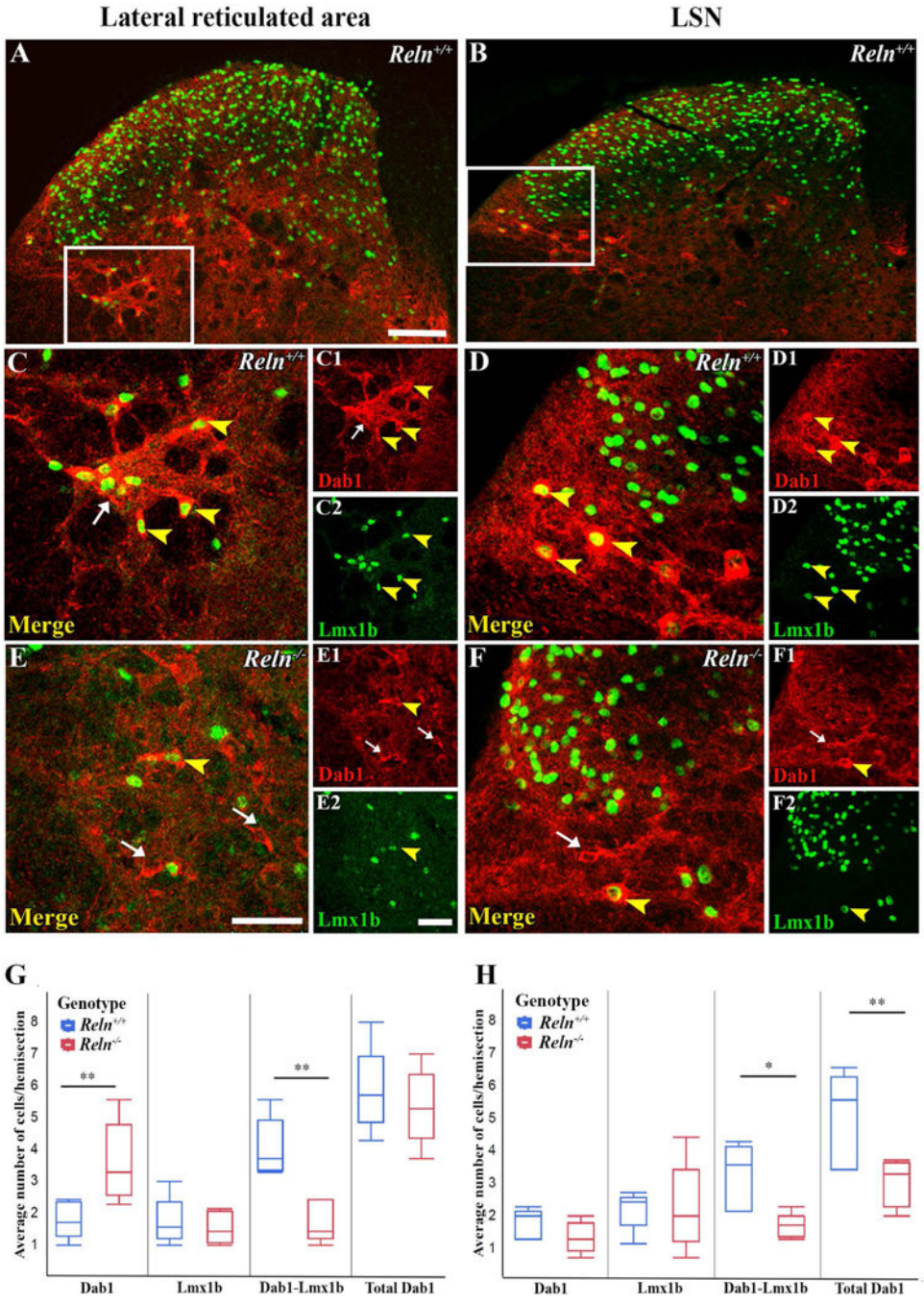

Figure 5. Lateral reticulated area and LSN: Dab1-Lmx1b-labeled cells are mispositioned in *Reln* mutants

A–F, Lumbar confocal images show that Dab1 (red) and Lmx1b (green) are co-expressed in *Reln*$^{+/+}$ (***A–D***) and *Reln*$^{-/-}$ (***E–F***) lateral reticulated area of lamina V (***A***, ***C***, ***E***, yellow arrowheads) and LSN (***B***, ***D***, ***F***, yellow arrowheads). Close to 70% of Dab1 neurons in both areas co-express Lmx1b. Single-labeled Dab1 cells are marked with white arrows. ***A***, ***C***, ***E***, Boxed area in ***A*** is enlarged in ***C*** and shows a more organized array of Dab1-Lmx1b neurons in *Reln*$^{+/+}$ than *Reln*$^{-/-}$ lateral reticulated area (***E***). ***B***, ***D***, ***F***, Boxed area of *Reln*$^{+/+}$ LSN is

enlarged in ***D*** and contains more Dab1-Lmx1b-labeled cells than in *Reln*$^{-/-}$ LSN (***F***). ***G***, Fewer Dab1 only and more Dab1-Lmx1b-labeled cells are in *Reln*$^{+/+}$ than in *Reln*$^{-/-}$ lateral reticulated area. ***H***, More Dab1-Lmx1b-labeled and total Dab1 cells are seen in *Reln*$^{+/+}$ than *Reln*$^{-/-}$ LSN (n=5 mice per genotype). Scale bars: ***A***, ***B***, 100 μm; ***C–F***; ***C1-2***, ***D1-2***, ***E1-2***, ***F1-2***, 50 μm.

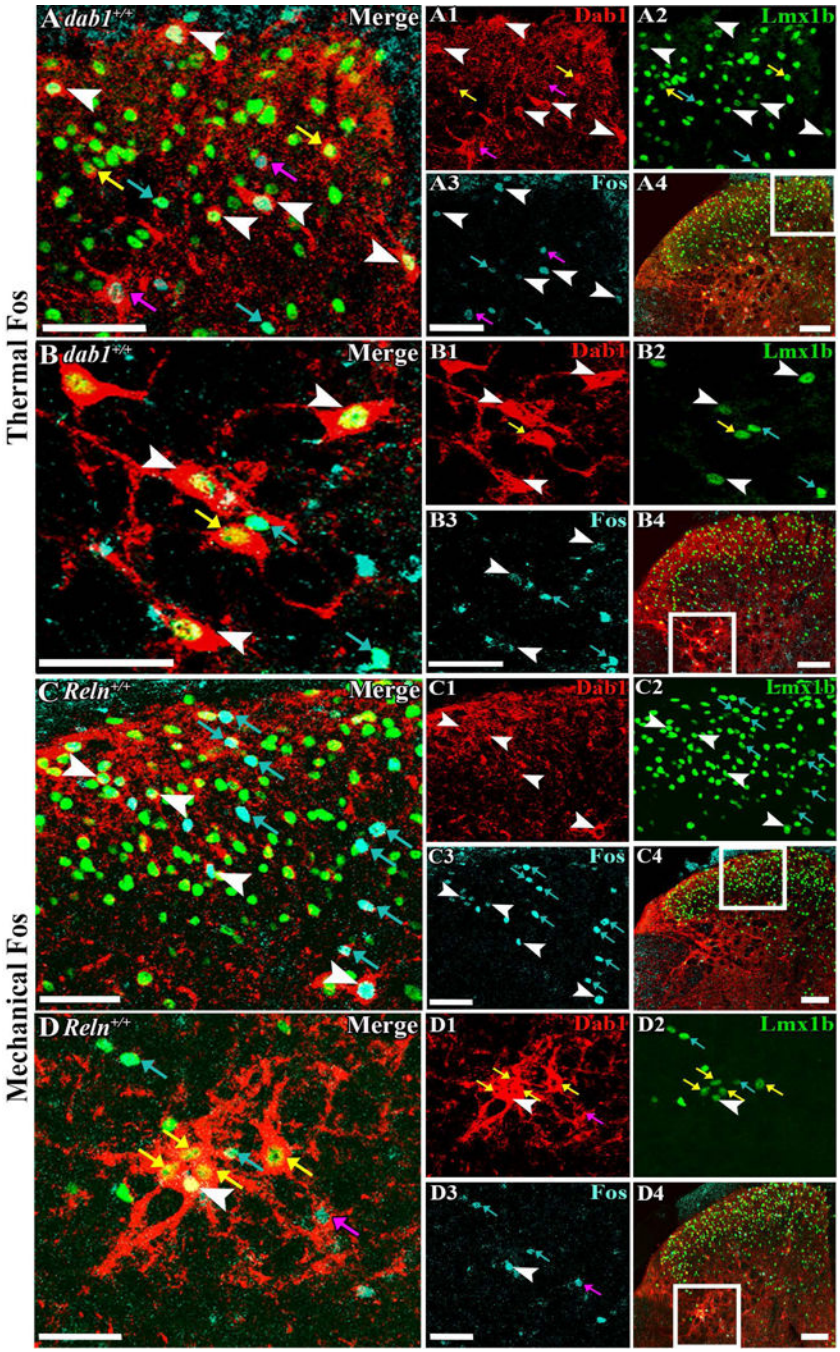

Figure 6. Noxious stimulation induced Fos expression in Dab1-Lmx1b neurons

Triple TSA immunofluorescence labeling showed that after both thermal (***A–B***) and mechanical stimulation (***C–D***), some Dab1 (red) and Lmx1b (green)-positive neurons express Fos (cyan) in *dab1*$^{+/+}$ (***A–B***) and *Reln*$^{+/+}$ (***C–D***) superficial dorsal horns (***A***, ***A1-4***, ***C***, ***C1-4***) and in the lateral reticulated area (***B***, ***B1-4***, ***D***, ***D1-4***). Boxed areas in ***A4–D4*** are enlarged in ***A–D***, respectively. Triple-labeled cells are marked with white arrowheads. Double-labeled Dab1-Fos (magenta), Lmx1b-Fos (cyan), and Dab1-Lmx1b (yellow) cells are marked with color-matched arrows. Heat and mechanical stimulation induced Fos in

medium to large-sized Dab1-Lmx1b neurons in the superficial dorsal horn and the lateral reticulated area. More Lmx1b neurons appeared to express Fos after mechanical stimulation especially in the superficial dorsal horn. Dab1-Lmx1b neurons in the lateral reticulated area appear as an organized array in wild-type mice (***B***, ***D***). Scale bars: ***A4***; ***B4***; ***C4***; ***D4***, 100 μm; ***A***; ***A1-3***; ***B***; ***B1-3***; ***C***; ***C1-3***; ***D***; ***D1-3***, 50 μm.

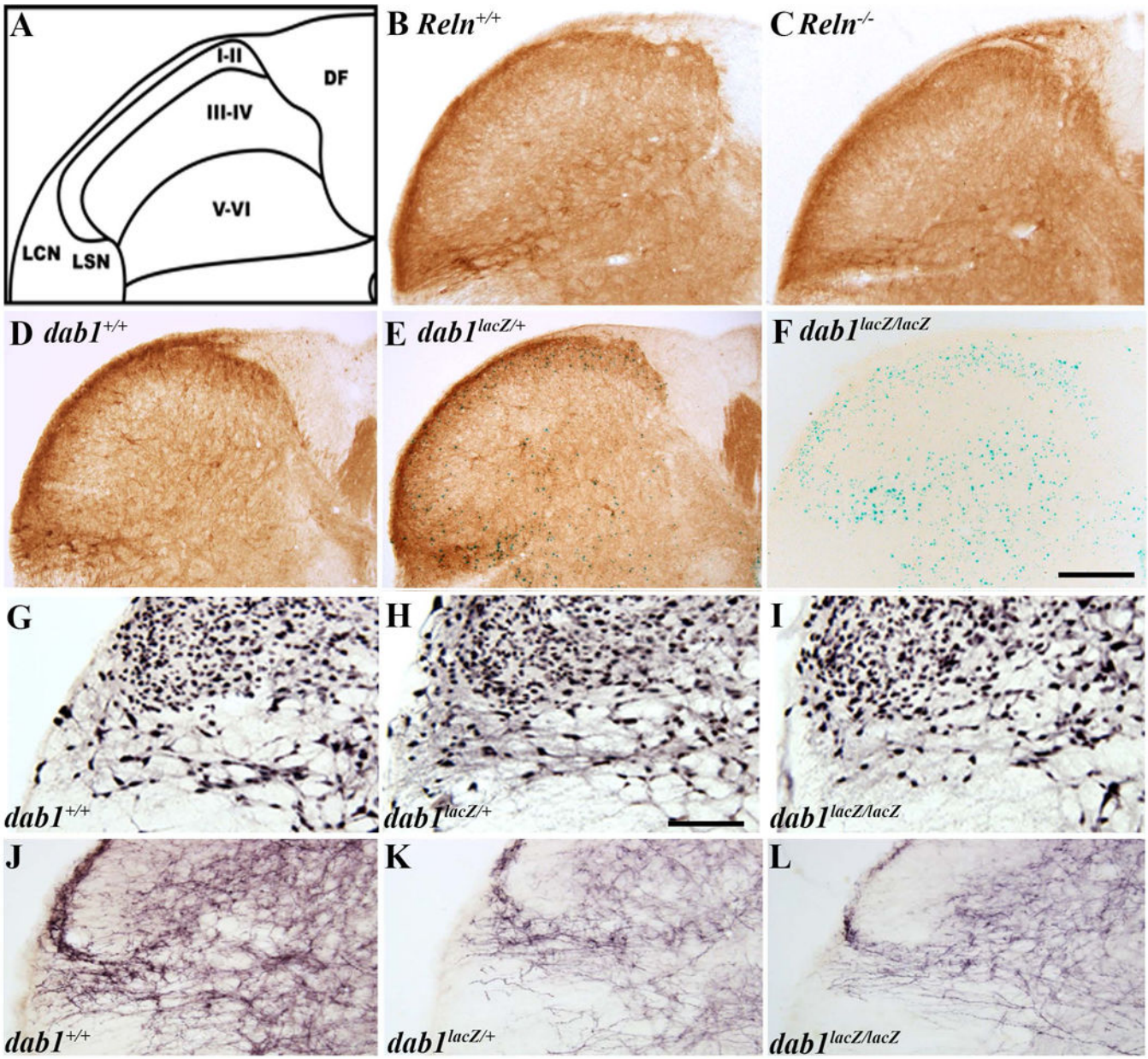

Figure 7. Lateral cervical nucleus: Neurons are mispositioned in Reelin pathway mutants

A, Schematic of the lateral cervical nucleus (LCN) found at levels C1-3. As there is no delineation between the LCN and LSN, they were analyzed together. ***B–C***, Dab1 expression in *Reln*$^{+/+}$ (***B***) and *Reln*$^{-/-}$ (***C***) cervical dorsal horn is concentrated in the superficial dorsal horn and LCN/LSN. ***D–F***, β-gal histochemistry followed by Dab1 immunoreaction reveals brown Dab1 protein (*dab1*$^{+/+}$, *dab1*$^{lacZ/+}$) and blue β-gal (*dab1*$^{lacZ/+}$, *dab1*$^{lacZ/lacZ}$) in the superficial dorsal horn and LCN/LSN. ***G–I***, The *dab1*$^{+/+}$ and *dab1*$^{lacZ/+}$ LCN/LSN contain about twice as many NeuN-labeled cells as *dab1*$^{lacZ/lacZ}$ mice (n=5 mice/genotype). ***J–L***, Neurons and their processes that express the Neurokinin-1 receptor show a compression in the *dab1*$^{lacZ/lacZ}$ (***L***) compared to *dab1*$^{+/+}$ (***J***) and *dab1*$^{lacZ/+}$ (***K***) LCN/LSN (n=3 mice/genotype). Scale bars: ***B–F***, 200 μm; ***G–L***, 100 μm.

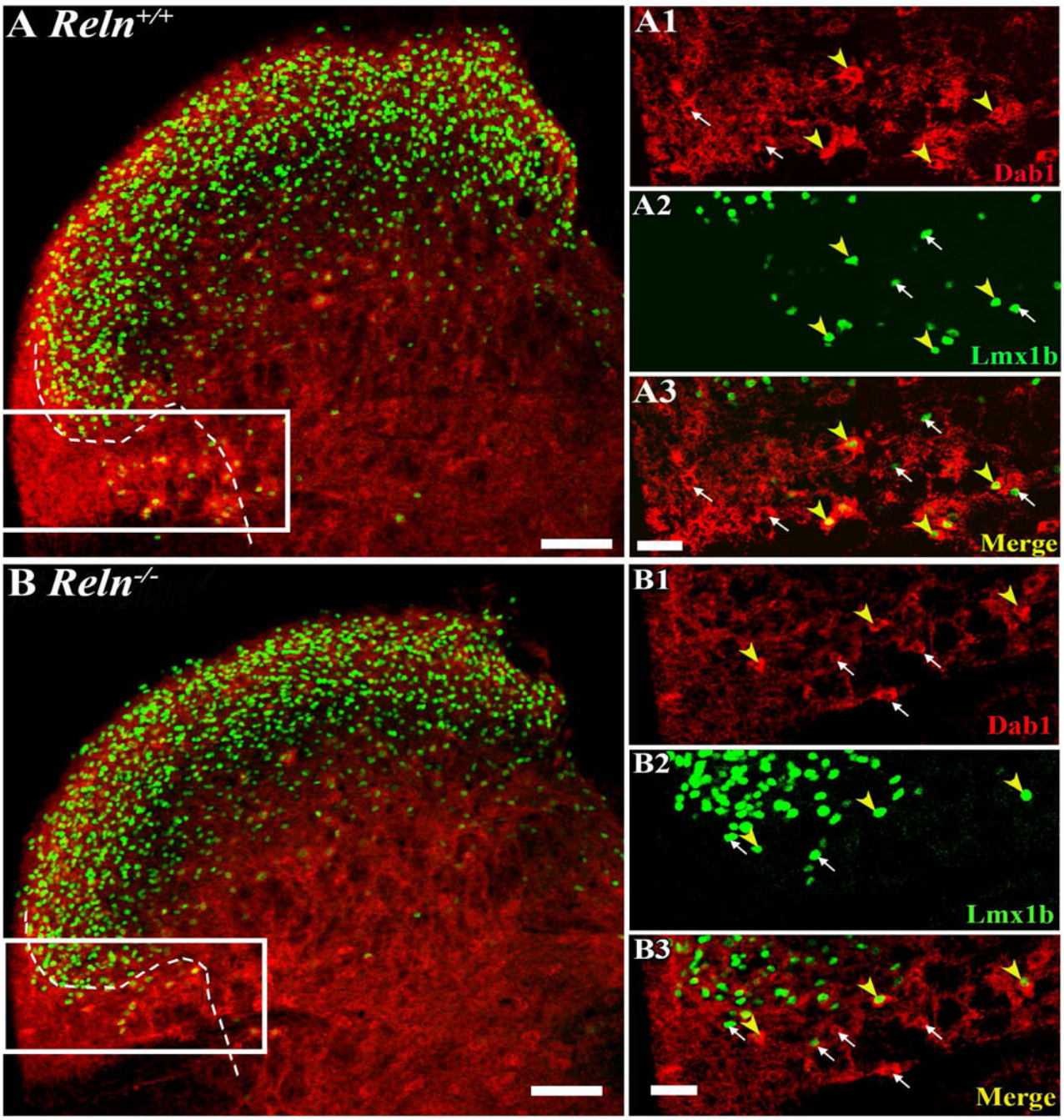

Figure 8. Lateral cervical nucleus: Dab1-Lmx1b neurons are mispositioned in *Reln* mutants

A–B, Confocal images of cervical level C2 sections of $Reln^{+/+}$ (***A***) and $Reln^{-/-}$ (***B***) dorsal horn. LCN/LSN is designated by a dashed line and boxed areas in ***A*** and ***B*** are enlarged in ***A1-3*** and ***B1-3***. White arrows mark single-labeled red Dab1 or green Lmx1b cells and yellow arrowheads indicate co-localization. About 50% of the Dab1-Lmx1b neurons are missing from $Reln^{-/-}$ LCN/LSN (n=5 mice/genotype). Scale bars: ***A***; ***B***, 100 μm; ***A1-3***; ***B1-3***, 50 μm.